



Equation of state and high-pressure stability of Fe₃P-schreibersite: Implications for phosphorus storage in planetary cores

Henry P. Scott,¹ Sabrina Huggins,¹ Mark R. Frank,² Steven J. Maglio,² C. David Martin,³ Yue Meng,⁴ Javier Santillán,⁵ and Quentin Williams⁶

Received 26 December 2006; revised 5 February 2007; accepted 14 February 2007; published 21 March 2007.

[1] We have collected in situ X-ray diffraction patterns of end-member Fe₃P-schreibersite in a diamond anvil cell to pressures of 30 GPa at 300 K. Some samples of Fe₃P were also laser heated at high pressure to temperatures of ~2000 K and examined following thermal quench. Below 8 GPa, variation of the schreibersite unit cell delineates a smooth pressure-volume curve corresponding to a second order Birch-Murnaghan equation of state with bulk modulus, K_{07} , of 159(1) GPa. Above 8 GPa, however, the schreibersite structure shows substantial stiffening, and an unidentified structure develops between 17 and 30 GPa; upon decompression to ambient pressure the schreibersite structure returns. Therefore, although ubiquitous in iron-rich meteorites, it is unlikely that schreibersite is the stable phosphorus-bearing phase in deep planetary cores.

Citation: Scott, H. P., S. Huggins, M. R. Frank, S. J. Maglio, C. D. Martin, Y. Meng, J. Santillán, and Q. Williams (2007), Equation of state and high-pressure stability of Fe₃P-schreibersite: Implications for phosphorus storage in planetary cores, *Geophys. Res. Lett.*, 34, L06302, doi:10.1029/2006GL029160.

1. Introduction

[2] (Fe, Ni)₃P-schreibersite is a component of nearly all iron meteorites [Wasson, 1974]. It has been used to assess both the origins and thermal history of host meteorites and the possible incorporation mechanisms for phosphorus in Earth. The characteristic amount of P in such meteorites varies between 0.2 and 1.1 wt% [Buchwald, 1975]. The exsolution rate of (Fe, Ni)₃P from α -(Fe, Ni)-kamacite has long been used as a proxy for the cooling rate of iron meteorites and their parent bodies [e.g., Randich and Goldstein, 1975; Hewins and Goldstein, 1977]. The P content in solid and liquid phases in the Fe-Ni-P, Fe-Ni-S and Fe-Ni-P-S-C systems has also been used to assess the partitioning of siderophile and light elements during the formation of iron meteorites [Chabot and Jones, 2003]. For differentiated meteoritic parent bodies, the ubiquity of schreibersite in

iron-rich meteorites implies that P partitions strongly into iron-rich material at modest pressures and high-temperatures. Moreover, schreibersite is far more abundant in meteorites than oxidized P-bearing minerals such as Ca₆(Mg, Fe)(PO₄)₆(PO₃OH)-whitlockite and Ca₅(PO₄)₃(OH, F, Cl)-apatite.

[3] If iron-rich meteorites are representative of the non-volatile composition of Earth's core, then the amount of P within iron-rich meteorites may represent a lower bound on the amount of P in this region. Thus, P may represent a minor, but not trace, constituent of Earth's core, with the most likely major components alloying with Fe in the deep Earth being H, C, O, Si and/or S [e.g., Birch, 1952; Ringwood, 1979; Poirier, 1994; Williams and Knittle, 1997; Scott et al., 2001; Li and Fei, 2003]. The crucial uncertainty in such bulk Earth compositional estimates lies in the amount of "volatile" elements likely to be present within Earth's core. The possible importance of minor constituents such as P is illustrated by the amount of lighter component sequestered in Earth's inner core.

[4] Seismic data and theoretical calculations suggest that Earth's inner core is composed of iron with ~5% of a lighter Fe-alloy component [Jephcoat and Olson, 1987; Stixrude et al., 1997]. Thus, the light-alloying components in Earth's inner core comprise only 0.5% of the total mass of Earth's core, or an amount comparable to those of minor constituents like P [e.g., Adler and Williams, 2005]. Fe₃P-type phases could thus be important in solid iron-alloy systems, such as Earth's inner core, at high pressures. For example, an additional light alloying phase, Fe₃S, is isostructural with Fe₃P and has been shown to form in the Fe-FeS system at temperatures >1000 K at 21 GPa [Fei et al., 2000]. It is possible that a solid solution may exist between these two isostructural compounds. However, since tetragonal Fe₃P-schreibersite has not been investigated under deep Earth conditions, it is unknown whether this phase is stable at high pressures and temperatures; moreover, its elasticity is unconstrained. Here we investigate end-member Fe₃P-schreibersite using synchrotron based X-ray diffraction to determine its isothermal equation of state. Furthermore, we have collected high pressure diffraction data following double-sided laser heating both to thermally anneal stress gradients and also to investigate its high-temperature, high-pressure stability.

2. Experiment

[5] A sample of synthetic, -40 mesh, 99.5% pure (metals basis) Fe₃P-iron phosphide was obtained from Alfa Aesar. The bulk sample contained minor phases in addition to Fe₃P, most notably Fe₂P, but we were able to select an

¹Department of Physics and Astronomy, Indiana University, South Bend, Indiana, USA.

²Department of Geology and Environmental Geosciences, Northern Illinois University, Dekalb, Illinois, USA.

³Department of Geological Sciences, State University of New York at Stony Brook, New York, USA.

⁴High Pressure Collaborative Access Team, Carnegie Institution of Washington, Argonne, Illinois, USA.

⁵Department of Earth Sciences, Massachusetts Institute of Technology, Cambridge, Massachusetts, USA.

⁶Department of Earth Sciences, University of California, Santa Cruz, California, USA.

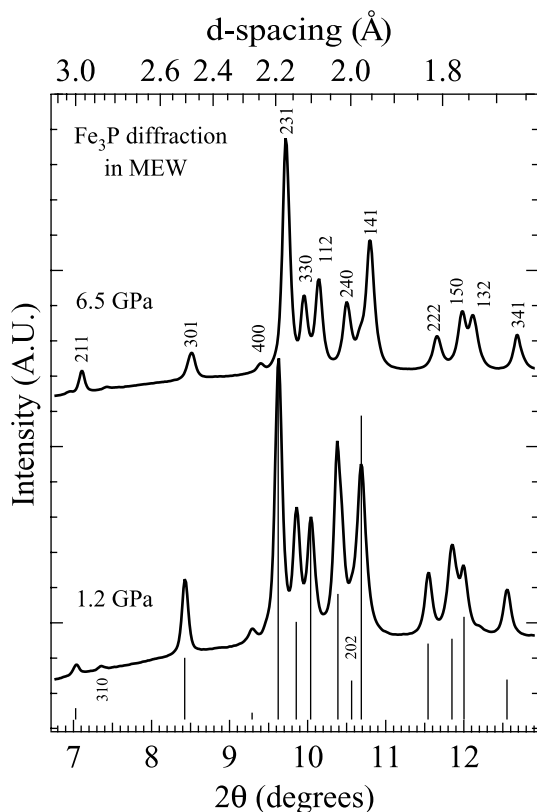


Figure 1. Representative in situ high-pressure diffraction of Fe_3P in MEW as a pressure-transmitting medium at 1.2 and 6.5 GPa. The vertical lines are the calculated diffraction positions based on our EoS at 1.2 GPa; corresponding hkl 's are indicated on the 6.5 GPa profile. The hkl 's written below the 1.2 GPa pattern were not consistently resolvable and were not used to determine lattice parameters. These patterns were collected at HP-CAT with a monochromatic energy of 0.3678 Å.

aliquot of nearly pure Fe_3P through visual observation and trial and error with powder X-ray diffraction. Our measured ambient pressure lattice parameters for this tetragonal structure (space group $I\bar{4}$, $Z = 8$) are as follows, with $1-\sigma$ uncertainties on the last digit shown parenthetically: $\mathbf{a} = 9.099(2)$ Å, $\mathbf{c} = 4.463(2)$ Å, and $V_0 = 369.5(2)$ Å³. These are in excellent agreement with the Joint Committee on Powder Diffraction Standards card #19-617: $\mathbf{a} = 9.100$ Å, $\mathbf{c} = 4.459$ Å, and $V_0 = 369.3$ Å³.

[6] Diamond Anvil Cells (DACs) with 350 μm culets and 150 μm sample chambers drilled in stainless steel gaskets were used to hold and compress samples for all X-ray measurements. We collected data at two X-ray beamlines of the Advanced Photon Source at Argonne National Lab: 13BM-D at GSECARS-CAT and 16ID-B at HP-CAT. Two-dimensional diffraction images were converted to one-dimensional profiles using FIT2D [Hammersley *et al.*, 1996].

2.1. 13BM-D at GSECARS-CAT

[7] We used monochromatic X-rays ($\lambda = 0.3344$ Å) and an MAR345 online imaging detector. We collected data at both ambient conditions and under compression to a maximum pressure of 7.4 GPa. A 16:3:1 volumetric ratio of

Methanol:Ethanol:Water (MEW) was used as a pressure transmitting medium for all measurements at elevated pressures. Pressure was measured using the ruby fluorescence technique [Mao *et al.*, 1978]. We detected diffraction from the two most intense peaks of Fe_2P in this experiment, but were able to unambiguously observe at least 8 reflections from the following 10 hkl 's in Fe_3P : (211), (301), (231), (330), (330), (112), (141), (222), (150) and (132). This data-set is referred to as **MEW-GSECARS**.

2.2. 16ID-B at HP-CAT

[8] These experiments also used monochromatic X-rays and an MAR345 detector, but utilized a slightly different wavelength ($\lambda = 0.3678$ Å). We conducted two compression studies. (1) For comparison with the GSECARS-CAT data we again used MEW as a pressure-transmitting medium, but extended our pressure range to 14.5 GPa. (2) To reduce shear stress above the point at which MEW is expected to freeze (~ 15 GPa [Fujishiro *et al.*, 1982]), we instead used NaCl coupled with double-sided laser heating after each change in pressure. We will refer to these data-sets as **MEW-HPCAT** and **NaCl-HPCAT**, respectively.

[9] We did not detect any Fe_2P in the **MEW-HPCAT** data-set and were able to track at least 11 of the following 12 hkl 's for all but the two highest pressure diffraction patterns: (211), (301), (400), (231), (330), (112), (240), (141), (222), (151), (132) and (341). Representative diffraction patterns from 1.2 and 6.2 GPa are shown in Figure 1. The diffraction peaks at 12.8 and 14.5 GPa were significantly broadened and reduced our ability to resolve individual peaks to 8 and 6 hkl 's, respectively.

[10] Our primary motivation for the laser heating experiment (**NaCl-HPCAT**) was to thermally anneal deviatoric stress, but this may also facilitate kinetically-impeded phase transitions if they occur. The laser heating system has been described previously by Meng *et al.* [2006]. The Fe_3P sample was loaded between two discs of pre-compressed NaCl to thermally insulate the sample from the diamond anvils. For pressure determination, we used both ruby fluorescence and the lattice parameter of NaCl, using the equation of state of Decker [1971]. We found that these results agreed to within 3%. We did not begin laser heating until the sample had been compressed to 10 GPa to avoid melting the NaCl; accordingly, the diffraction peaks at pressures below 10 GPa showed significant broadening and we do not include them in our analysis. We were careful to heat just enough to sharpen diffraction peaks and the blackbody radiation was just barely visible. Accordingly, temperatures were too low for reliable measurement, but we estimate that they were below ~ 1000 K. Notably, the ruby fluorescence profiles post laser heating showed no peak broadening relative to the ambient pressure spectrum. As with **MEW-HPCAT**, we see weak diffraction evidence for Fe_2P in this data-set in addition to NaCl. Nevertheless, we are able to clearly fit at least 6 of the following 7 hkl 's: (301), (231), (330), (112), (141), (150) and (132).

3. Results and Discussion

[11] Our experimental pressures and calculated lattice parameters and unit cell volumes are shown in Table 1.

Table 1. Summary of Lattice Parameters and Unit Cell Volumes for Fe₃P as a Function of Pressure for Three Different Experimental Runs^a

Data-Set	P (GPa)	a (Å)	c (Å)	V (Å ³)
MEW-HPCAT	Ambient	9.099(2)	4.463(2)	369.5(2)
MEW-GSECARS	0.2(1)	9.098(1)	4.460(1)	369.2(1)
MEW-GSECARS	0.5(1)	9.092(3)	4.454(2)	368.2(3)
MEW-GSECARS	0.7(1)	9.094(1)	4.454(1)	368.3(2)
MEW-HPCAT	1.2(1)	9.080(2)	4.448(1)	366.7(2)
MEW-GSECARS	2.4(1)	9.063(3)	4.436(2)	364.4(3)
MEW-GSECARS	2.7(1)	9.056(4)	4.434(1)	363.6(3)
MEW-HPCAT	3.5(1)	9.037(1)	4.427(0)	361.6(1)
MEW-HPCAT	3.7(1)	9.032(2)	4.429(1)	361.3(2)
MEW-GSECARS	4.4(1)	9.023(1)	4.419(1)	359.8(1)
MEW-HPCAT	5.2(2)	9.013(1)	4.412(1)	358.4(1)
MEW-HPCAT	5.6(2)	9.004(1)	4.410(1)	357.6(1)
MEW-GSECARS	6.2(2)	8.994(2)	4.408(2)	356.6(2)
MEW-HPCAT	6.5(2)	8.986(3)	4.402(2)	355.5(3)
MEW-GSECARS	6.8(2)	8.988(2)	4.402(2)	355.6(2)
MEW-GSECARS	7.4(2)	8.976(2)	4.394(1)	354.1(2)
MEW-HPCAT	9.1(3)	8.959(2)	4.385(3)	351.9(3)
MEW-HPCAT	9.5(3)	8.943(3)	4.389(3)	351.0(3)
NaCl-HPCAT	9.9(3)	8.937(2)	4.395(1)	351.1(2)
MEW-HPCAT	10.0(3)	8.952(3)	4.378(4)	350.8(4)
MEW-HPCAT	11.0(3)	8.943(3)	4.374(3)	349.8(3)
NaCl-HPCAT	12.3(3)	8.919(5)	4.379(8)	348.3(7)
MEW-HPCAT	12.4(4)	8.914(3)	4.371(3)	347.3(3)
MEW-HPCAT	12.8(4)	8.905(6)	4.363(8)	346.0(8)
NaCl-HPCAT	13.6(4)	8.888(5)	4.374(8)	345.5(8)
MEW-HPCAT	14.5(4)	8.919(12)	4.329(10)	344.3(12)
NaCl-HPCAT	15.5(5)	8.870(2)	4.373(2)	344.1(2)
NaCl-HPCAT	16.7(5)	8.839(6)	4.350(4)	339.9(6)

^aExperimental runs are described in text. 1- σ uncertainties on the last digit are shown parenthetically. The ambient pressure data are labeled as **MEW-HPCAT** because they are from the sample used for that run, but the data were taken prior to loading the MEW pressure-transmitting medium.

There is excellent agreement between **MEW-GSECARS** and **MEW-HPCAT** in the pressure range over which they overlap (i.e. to 8 GPa), and a plot of unit cell volume as a function of pressure is shown in Figure 2. The unit cell volume data from **MEW-HPCAT** show a discontinuity near 8 GPa with a decrease in compressibility and increased scatter above this pressure. We do not believe that this phenomenon is related to a loss of hydrostaticity in the MEW pressure-transmitting medium because the data from **NaCl-HPCAT** agree with these volumes very well. Furthermore, although it has been suggested that MEW may freeze below the previously-published pressure of 14.5 GPa [Fujishiro *et al.*, 1982], a recent study indicates that the glass transition may be near 10.5 GPa [Angel *et al.*, 2007], which is well above our observed discontinuity between 7 and 9 GPa.

[12] We do not have a definitive explanation for the abrupt change in compressibility, but we speculate that it may result from a transition in electronic state from high-spin to low-spin. This phenomenon has been previously documented in Fe₃S [Lin *et al.*, 2004a] and Fe₃C [Lin *et al.*, 2004b] at pressures of 21 and 25 GPa, respectively. Notably, electronic transitions have been shown to affect elasticity at lower pressures as well; for example, an abrupt change in dK/dP has been documented in Fe₆₄Ni₃₆ at 3.1 GPa [Decremps and Nataf, 2004]. Confirmation of this hypothesis will require in situ synchrotron Mössbauer spectroscopy and will be the subject of a future study.

[13] Due to our observed discontinuity in unit cell volume, we have used only the data below 8 GPa to determine the equation of state (EoS) for Fe₃P-schreibersite. We derive a 300 K bulk modulus (K_{0T}) of 159(1) GPa and a fit volume of 369.5(1) Å³ from a 2nd order Birch-Murnaghan equation

of state [Birch, 1978]. This value is slightly lower than that of α -Fe (163(5) GPa with a fit $\frac{dK}{dP}$ of 5.5 [Takahashi and Bassett, 1968]) and very similar to that of Fe₃S (156(7) with a fit $\frac{dK}{dP}$ of 3.8 [Seagle *et al.*, 2006]). An attempt to fit all P-V data (i.e., ambient to 16 GPa) with a 3rd order EoS yielded unsatisfactory results and required an unreasonably high $\frac{dK}{dP}$ of 8.5.

[14] The inset in Figure 2 shows the ratio of lattice parameters, $\frac{c}{a}$, as a function of pressure. This ratio remains nearly constant at 0.490 below 8 GPa with very little scatter. Above 8 GPa we observe increased scatter and a slightly positive slope for **NaCl-HPCAT**; $\frac{c}{a}$ approaches 0.493 by 16 GPa. A linear fit to the data in this region yields a slope of $2.9(9) \times 10^{-4}/\text{GPa}$, and by extrapolation we would expect $\frac{c}{a}$ to reach 0.5 at ~ 42 GPa, and the structure to become cubic at these conditions. Yet, this effect is not observed in **MEW-HPCAT**; indeed, our highest pressure datum in MEW (14.6 GPa) suggests a drop in $\frac{c}{a}$ to 0.485. Although we cannot rule out a potential effect from laser heating, we attribute this to anisotropic strain due to the freezing of MEW and believe that the observed increase with pressure in **NaCl-HPCAT** is real. We expect preferential alignment to orient crystallites with their long axis (i.e., **a**) perpendicular to the principal stress component of the DAC once the glass transition has been reached in MEW. This should preferentially compress **c** relative to **a** and accordingly produce a decrease in $\frac{c}{a}$.

[15] We are unable to index the unit cell for Fe₃P-schreibersite above 17 GPa. All of our data in this pressure regime are from **NaCl-HPCAT** and therefore include diffraction lines from NaCl. Furthermore, by 25 GPa our diffraction patterns contain both the B1 and B2 structures of NaCl; we observe the B2 phase metastably at 25 GPa and 300 K due to its stability under laser-heating, and resultant

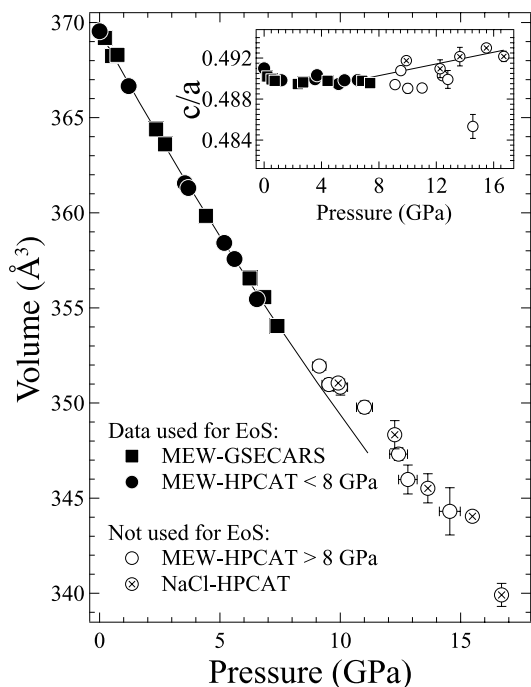


Figure 2. Pressure-volume data for Fe_3P . Only data below 8 GPa were used to determine the EoS: $K_{0T} = 159(1)$ GPa, $\frac{dK}{dP} \equiv 4$. A discontinuity in compressibility is observed above 8 GPa; notably, two different data-sets (one in MEW and the other, NaCl) reflect this phenomenon. (inset) Variation in the ratio of unit cell lattice parameters, a and c , as a function of pressure. $\frac{c}{a}$ remains essentially constant until 8 GPa, but a positive slope is observed above this pressure. The datum near 14 GPa is explained in the text.

quenching. Due to reflections from multiple phases and a gradual progression of the phase transition, we are unable to conclusively determine the structure of the new phase. Even at our highest pressure, 30 GPa, we still see evidence for the most intense Fe_3P diffraction lines (i.e., (231) and (141)).

[16] However, we speculate that an AuCu_3 -type structure is likely, as has been theoretically-predicted for Fe_3S at high pressure [Sherman, 1995]. At 30 GPa we observe an unambiguous new diffraction line which is at a d-spacing of 2.02 Å. The most intense reflection, (111), from the AuCu_3 -type structure is expected at this d-spacing for a lattice parameter, a , near 3.5 Å. This implies a unit cell volume of $\sim 40 \text{ Å}^3$; from our measured EoS for Fe_3P -schreibersite, we would expect a unit cell volume of 319.6 Å^3 at 30 GPa. However, schreibersite has eight formula units per unit cell versus only one for the AuCu_3 -type structure making the volumes compatible.

[17] We did not laser heat during decompression, but found that the original schreibersite structure returned on decompression to ambient pressure. Accordingly, we can rule out a chemical reaction occurring between the sample and the NaCl pressure-transmitting medium, and it is very unlikely that a dissociation reaction between Fe and P occurred.

4. Conclusions

[18] We have measured the 300 K equation of state for Fe_3P -schreibersite to 8 GPa. Above this pressure we

observed an abrupt change in compressibility followed by a reversible structural transformation which gradually progresses between 17 and 30 GPa. Therefore, if phosphorus is present in Earth's core, it is not in the schreibersite structure. This observation may place a constraint on the size of the protoplanetary bodies from which schreibersite inclusions are derived. Although the structural transformation is reversible, the associated change in density could produce textural evidence if the body were large enough to induce the transformation to the high-pressure phase.

[19] The abundance of Fe_3P in iron meteorites indicates that P is a likely candidate as a light-alloying component in liquid outer cores of most planetary bodies. For small and relatively cooler bodies such as Ganymede, where crystallization of the core may have proceeded to a greater extent than on Earth, P-enrichment in any liquid outermost core could be extensive [Schubert *et al.*, 2004]. Indeed, for cores that are $\sim 80\%$ crystallized, the abundance of P in the residual liquid could be near 5 wt%: an amount approaching that of the light alloying element in Earth's core. In the newly defined group IIG iron meteorites, schreibersite occupies $\sim 15\%$ of their area and as the most P-rich iron meteorites [Bartoschewitz, 2003], they may represent the differentiate from a largely solidified core. Given that Fe_3P is 15% by weight phosphorus, we would expect that the final $\sim 10\%$ of a solidifying core of a small cold body to be composed dominantly of Fe_3P . In the case of Mars, recent geodetic data appear to require that at least the outer portions of Mars' core are liquid [Yoder *et al.*, 2003; Zharkov and Gudkova, 1997; Gudkova and Zharkov, 1996]. Whether a large inner core exists on Mars is unknown: if such a feature exists, then P may be an abundant component of the liquid portion of the outer core.

[20] Finally, since the structural transition we observe is reversible upon decompression, it is likely that phosphorus is indeed stable within an iron phosphide structure until at least 30 GPa. If this stability continues to core pressures, it is likely that most primordial phosphorus is contained within Earth's core and that biochemically important phosphorus derived from iron meteorites was delivered to a corrosive aqueous environment during late stage accretion [Pasek and Lauretta, 2005]. Our study indicates that Fe_3P will have a minimal effect on the density, elasticity and likely anisotropy of planetary cores of objects such as the Moon, the top of Mercury's core (if solid) and the Galilean satellites. Fe_3P 's elasticity is almost identical to that of iron, and its density is $\sim 5\%$ less. Accordingly, phosphorus is likely to be a seismically invisible component of planetary cores.

[21] **Acknowledgments.** We are indebted to V. Prakapenka at GSECARS-CAT for experimental advice. We also thank N. Boctor and M. Pasek for helpful discussions regarding Fe_3P starting material. Use of the HPCAT facility was supported by U.S. Department of Energy (DOE)-Basic Energy Sciences, DOE-National Nuclear Security Administration, NSF, Department of Defense-Tank-Automotive and Armaments Command, and the W.M. Keck Foundation. This research was partially supported by NSF grant EAR-0310342 (JDS and QW). S. Huggins gratefully acknowledges financial assistance from the IUSB SMART program.

References

Adler, J. F., and Q. Williams (2005), A high-pressure X-ray diffraction study of iron nitrides: Implications for Earth's core, *J. Geophys. Res.*, *110*, B01203, doi:10.1029/2004JB003103.

- Angel, R. J., M. Bujak, J. Zhao, G. Dieggo Gatta, and S. D. Jacobsen (2007), Effective hydrostatic limits of pressure media for high-pressure crystallographic studies, *J. Appl. Crystallogr.*, *40*, 26–32.
- Bartoschewitz, R. (2003), Wu-chu-mu-ch'in—A complex iron meteorite from China with relation to Bellsbank and Britstown, paper presented at 66th Annual Meeting, Meteorit. Soc., Münster, Germany, 28 Jul. to 1 Aug.
- Birch, F. (1952), Elasticity and constitution of the Earth's interior, *J. Geophys. Res.*, *57*, 227–286.
- Birch, F. (1978), Finite strain isotherm and velocities for single-crystal and polycrystalline NaCl at high pressures and 300 degrees K, *J. Geophys. Res.*, *83*, 1257–1268.
- Buchwald, V. (1975), *Handbook of Iron Meteorites, Their History, Distribution, Composition, and Structure*, Univ. of Calif. Press, Berkeley.
- Chabot, N., and J. Jones (2003), The parameterization of solid metal-liquid metal partitioning of siderophile elements, *Meteorit. Planet. Sci.*, *38*, 1425–1436.
- Decker, D. (1971), High-pressure equation of state for NaCl, KCl, and CsCl, *J. Appl. Phys.*, *42*, 3239–3244.
- Decremps, F., and L. Nataf (2004), Abrupt discontinuity of the bulk modulus pressure dependence in Fe₆₄Ni₃₆, *Phys. Rev. B*, *92*, 157204, doi:10.1103/PhysRevLett.92.157204.
- Fei, Y., J. Li, C. Bertka, and C. Prewitt (2000), Structure type and bulk modulus of Fe₃S, a new iron-sulfur compound, *Am. Mineral.*, *85*, 1830–1833.
- Fujishiro, I., G. Piermarini, S. Block, and R. Munro (1982), Viscosities and glass transition pressures in the methanol-ethanol-water system, in *High Pressure Research in Science and Industry*, edited by C. M. Backman, T. Johannson, and L. Tegner, pp. 608–611, Arkitektkopia, Uppsala, Sweden.
- Gudkova, T., and V. Zharkov (1996), The exploration of Martian interiors using the spheroidal oscillation method, *Planet. Space Sci.*, *44*, 1223–1230.
- Hammersley, A., S. Svensson, M. Hanfland, A. Fitch, and D. Häusermann (1996), Two-dimensional detector software: From real detector to idealized image or two-theta scan, *High Pressure Res.*, *14*, 235–248.
- Hewins, R., and J. Goldstein (1977), Cooling rates for lunar samples determined with a diffusion model for phosphide exsolution, *Proc. Lunar Sci. Conf.*, *8th*, 1625–1638.
- Jephcoat, A., and P. Olson (1987), Is the inner core of the Earth pure iron?, *Nature*, *82*, 332–335.
- Li, J., and Y. Fei (2003), Experimental constraints on core composition, in *The Mantle and Core*, edited by R. Carlson, pp. 521–546, Elsevier, New York.
- Lin, J., Y. Fei, W. Sturhahn, J. Zhao, H. Mao, and R. Hemley (2004a), Magnetic transition and sound velocities of Fe₃S at high pressure: Implications for Earth and planetary cores, *Earth Planet. Sci. Lett.*, *226*, 33–40.
- Lin, J., V. Struzhkin, H. Mao, R. Hemley, P. Chow, M. Hu, and J. Li (2004b), Magnetic transition in compressed Fe₃C from X-ray emission spectroscopy, *Phys. Rev. B*, *70*, 212405, doi:10.1103/PhysRevB.70.212405.
- Mao, H., P. Bell, J. Shaner, and D. Steinberg (1978), Specific volume measurements of Cu, Mo, Pd, and Ag and calibration of the ruby R₁ fluorescence pressure gauge from 0.06 to 1 Mbar, *J. Appl. Phys.*, *49*, 3276–3283.
- Meng, Y., G. Shen, and H. Mao (2006), Double-sided laser heating system at HPCAT for in situ X-ray diffraction at high pressures and high temperatures, *J. Phys. Condens. Matter*, *18*, S1097–S1103.
- Pasek, M., and D. Lauretta (2005), Aqueous corrosion of phosphide minerals from iron meteorites: A highly reactive source of prebiotic phosphorus on the surface of the early Earth, *Astrobiology*, *5*, 515–535.
- Poirier, J. P. (1994), Light elements in the Earth's outer core: A critical review, *Phys. Earth Planet. Inter.*, *85*, 319–337.
- Randich, E., and J. Goldstein (1975), Nonisothermal finite diffusion-controlled growth in ternary systems, *Metall. Mater. Trans. A*, *6*, 1553–1560.
- Ringwood, A. E. (1979), *Origin of the Earth and Moon*, Springer, New York.
- Schubert, G., J. Andersen, T. Spohn, and W. McKinnon (2004), Interior composition, structure and dynamics of the satellites, in *Jupiter: The Planet, Satellites and Magnetosphere*, edited by F. Bagenal, T. Dowling, and W. McKinnon, pp. 281–306, Cambridge Univ. Press, New York.
- Scott, H. P., Q. Williams, and E. Knittle (2001), Stability and equation of state of Fe₃C to 73 GPa: Implications for carbon in the Earth's core, *Geophys. Res. Lett.*, *28*, 1875–1878.
- Seagle, C. T., A. J. Campbell, D. L. Heinz, G. Shen, and V. B. Prakapenka (2006), Thermal equation of state of Fe₃S and implications for sulfur in Earth's core, *J. Geophys. Res.*, *111*, B06209, doi:10.1029/2005JB004091.
- Sherman, D. (1995), Stability of possible Fe-FeS and Fe-FeO alloy phases at high pressure and the composition of the Earth's core, *Earth Planet. Sci. Lett.*, *132*, 87–98.
- Stixrude, L., E. Wasserman, and R. Cohen (1997), Composition and temperature of Earth's inner core, *J. Geophys. Res.*, *102*, 24,729–24,739.
- Takahashi, T., and W. A. Bassett (1968), Isothermal compression of the alloys of iron up to 300 kbar at room temperature: Iron-nickel alloys, *J. Geophys. Res.*, *73*, 4717–4725.
- Wasson, J. (1974), *Meteorites: Classification and Properties*, Springer, New York.
- Williams, Q., and E. Knittle (1997), Constraints on core chemistry from the pressure dependence of the bulk modulus, *Phys. Earth Planet. Inter.*, *100*, 49–59.
- Yoder, C., A. Konopliv, D. Yuan, E. Standish, and W. Folkner (2003), Fluid core size of Mars from detection of the solar tide, *Science*, *300*, 299–303.
- Zharkov, V., and T. Gudkova (1997), On the dissipative factor of the Martian interiors, *Planet. Space Sci.*, *45*, 401–407.

M. R. Frank and S. J. Maglio, Department of Geology and Environmental Geosciences, Northern Illinois University, Davis Hall 312, Normal Road, Dekalb, IL 60115, USA.

S. Huggins and H. P. Scott, Department of Physics and Astronomy, Indiana University, South Bend, 1700 Mishawa Avenue, South Bend, IN 46634, USA. (hpscott@iusb.edu)

C. D. Martin, Department of Geological Sciences, SUNY at Stony Brook, Stony Brook, NY 11794, USA.

Y. Meng, High Pressure Collaborative Access Team, Carnegie Institution of Washington, Argonne, IL 60439, USA.

J. Santillán, Department of Earth Sciences, Massachusetts Institute of Technology, Cambridge, MA 02139, USA.

Q. Williams, Department of Earth Sciences, University of California, Santa Cruz, 1156 High Street, Santa Cruz, CA 95064, USA.